Adaptive modulation system for liquid crystal phase modulator

Bin Zhang (张 彬), Shiyu Liu (刘诗雨), Xianzhu Tang (唐先柱), and Jian'gang Lu (陆建钢)*

Department of Electronic Engineering and National Engineering Lab for TFT-LCD Materials and Technologies,
Shanghai Jiao Tong University, Shanghai 200240, China
*Corresponding author: lujg@sjtu.edu.cn

An adaptive modulation system for a liquid crystal (LC) phase modulator is demonstrated. The phase retardation may be modulated by resetting the driving voltage automatically by matching the measured and ideal transmittance of an LC cell sandwiched by crossed polarizers. By using this system, an LC phase modulator can get a low error function of 0.25% in a short modulation time, which is less than the 10% obtained using a conventional modulation method.

OCIS codes: 060.5060, 160.3710.
doi: 10.3788/COL201614.090604.

Phase modulators are playing a more and more important role in modern optics. They can be widely applied in many fields, such as optical tomography[1], digital holography[2], spatial filtering[3], optical communications[4–7], optical manipulation[8,9], optical microfibers[10], and optical fiber sensing[11]. Due to the electric-control birefringence, liquid crystal (LC) devices are becoming one of the most competitive candidates for phase modulators. To improve the performance of the LC phase modulator, multi-electrode structures were introduced to match the ideal refractive index profile, as it makes different LC molecular orientation on different electrode[12–15]. Although the response time of LC is usually a few milliseconds, the time of conventional modulation process is mainly determined by three steps: (1) estimate the phase retardation profile to see if it is good or not, (2) decide how to revise a set of driving voltages on electrodes, and (3) manually reset the driving voltage on all electrodes. To reach its designed performance, a multi-electrode LC device needs to repeat the phase modulation process mentioned above at least dozens of times. Therefore, the tedious and complex modulation process takes at least several hours. The refractive index profile of an LC phase modulator cannot be illustrated directly in the modulation process, but only evaluated indirectly in the application by its performance.

In this Letter, an adaptive modulation system was proposed to yield a refractive index profile that matches the ideal one automatically. With this system, the refractive index profile can be real-time evaluated, and the modulation process can be efficiently shortened to 10% of that by using a conventional modulation method.

Firstly, a typical LC cell sandwiched by a polarizer and an analyzer is shown in Fig. 1. The relationship between the incident light intensity (I_0) and the emergent light intensity (I) can be expressed as Eq. (1)[16], when the polarization directions of the polarizer and analyzer are orthogonal,

$$T = \frac{I}{I_0} = \frac{1}{2}\sin^2(2\beta)\sin^2\left(\frac{\pi(n_{\text{eff}} - n_o)d}{\lambda}\right), \qquad (1)$$

where T is the transmittance, β is the polarization directions of the polarizer, d is the cell gap of the LC phase modulator, and n_o and n_{eff} are the ordinary refractive index and the effective refractive index of the LC, respectively. If β is set to $\pi/4$, which leads to the maximum T, Eq. (1) can be given by

$$T = \frac{I}{I_0} = \frac{1}{4}\left(1 - \cos\left(\pi \cdot \frac{2(n_{\text{eff}} - n_o)d}{\lambda}\right)\right). \qquad (2)$$
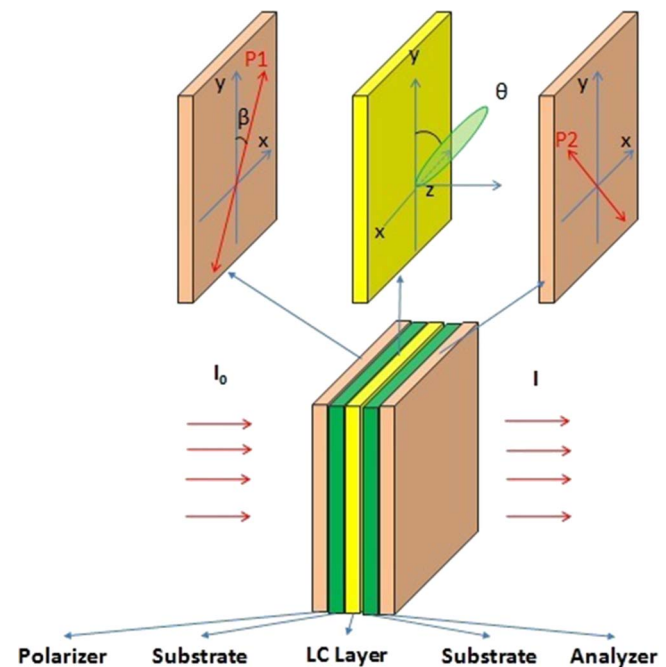

Fig. 1. Typical LC phase modulator sandwiched by polarizer and analyzer.

As the emergent light intensity versus n_{eff} corresponds to a cosine function, the transmittance will change periodically as n_{eff} changes linearly. For a multi-electrode structure LC phase modulator, a series of variable driving voltages is applied on the electrodes to induce a refractive index profile of LC molecules[17], and the distribution of the light intensity can be received by a CCD camera behind the analyzer. Therefore, the driving voltage can be modulated by comparing the measured transmittance distribution data with the ideal distribution, which can be calculated by Eq. (2) with the designed refractive index profile.

The configuration and the operating principle of the adaptive modulation system are shown in Figs. 2 and 3, respectively. A collimated light passes through two crossed polarizers with the sandwiched electrically controlled LC cell and then through a magnifying lens to the CCD camera, which is used to record the light intensity distribution data. The computer will decide whether the transmittance distribution is qualified by comparing the transmittance difference between the measured one and the ideal one with a threshold value. The transmittance difference can be calculated by

$$\text{MAPE} = \frac{1}{n} \sum_{1}^{n} \left| \frac{T_i - T_{io}}{T_{\text{max}}} \right|, \qquad (3)$$

where MAPE is the acronym for mean absolute percentage error, n is the number of sample points, T_i is the measured transmittance, T_{io} is the ideal transmittance,
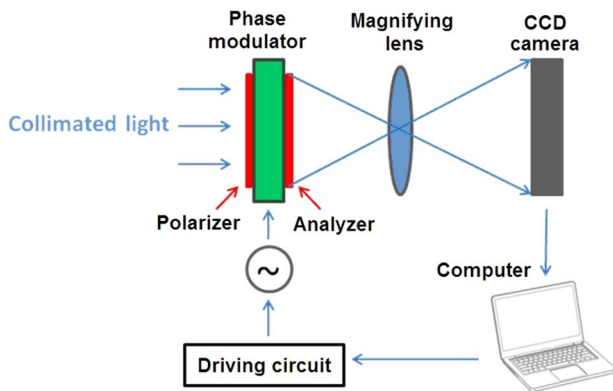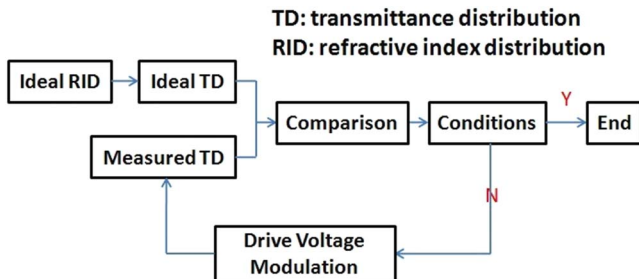
and T_{max} is the maximum of the ideal transmittance. If MAPE is smaller than the threshold value, the modulation process will stop and a set of driving voltages will be recorded as the result. Otherwise, the computer will continuously control the driving circuit to apply renewed driving voltages to the multi-electrode of the LC cell. Therefore, the driving voltage modulation process can be simplified with the adaptive system.
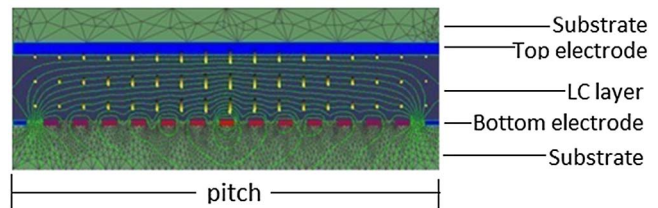
The adaptive modulation was used to modulate the driving voltages of an LC phase modulator. The LC phase modulator is shown in Fig. 4(a), and its structure is shown in Fig. 4(b). The cell gap of the LC modulator was 12.9 μm, and pitch of the LC modulator composed of 14 electrodes was 144.8 μm. Different sets of the driving voltages may be input on the electrodes to change the phase distribution periodically in the LC modulator. The extraordinary refractive index and ordinary refractive index of the LC were 1.805 and 1.524, respectively.

The LC phase modulator was configured into the adaptive modulation system. By using the ideal refractive index distribution of the optical phase modulator, the ideal transmittance distribution could be figured out according to Eq. (2), as shown in Fig. 5(a). A series of threshold values (5%, 10%, and 20%) for MAPE was set to initialize the adaptive system.

In order to ensure the modulator image through the magnifying lens to the CCD uniformly, we need to choose the position for modulator in three steps: (1) put the CCD and magnifying lens on the primary optical axis. The distance between the CCD and magnifying lens is determined by the designed amplification factor of the magnifying lens. In the experiment, we set the distance as about 15 times the magnifying lens focal distance. (2) Along the primary optical axis, move a small object with high brightness until the CCD shows the magnified image clearly.

Fig. 2. Configuration of the adaptive modulation system.

Fig. 3. Operating principle of the adaptive modulation system.

(a)

(b)

Fig. 4. (a) Picture of the LC phase modulator and driving board. (b) Structure of the LC phase modulator in one pitch.
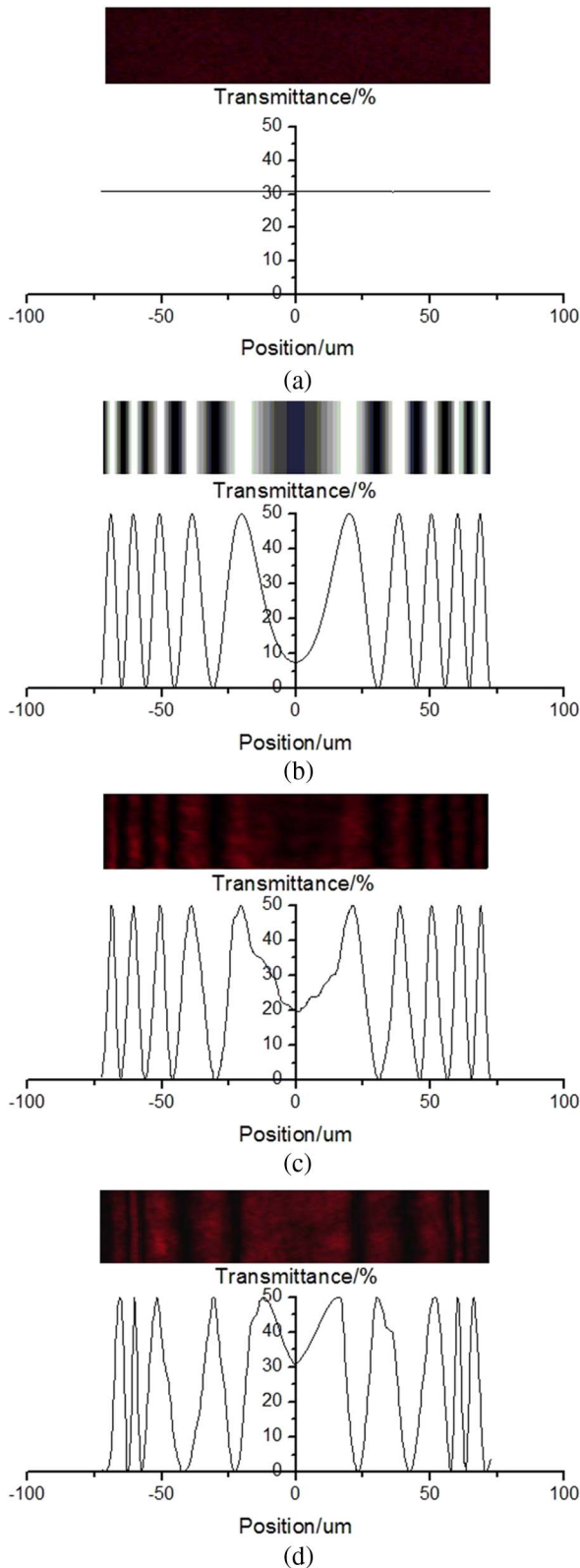
(a)

(b)

(c)

(d)

Fig. 5. Two-dimensional image and transmittance distribution. (a) Measurement result of luminance distribution and transmittance distribution without voltage. (b) Simulation result of luminance distribution and transmittance distribution. Measurement result of luminance distribution and transmittance distribution with voltage (c) before modulation and (d) after modulation.

Then, mark the position of the object. (3) Put the modulator on the marked position.

Before the experiment, the transmittance line obtained by the camera without any voltage on the modulator is achieved, as shown in Fig. 5(a). According to Fig. 5(a), we can see the uniformity of the transmittance is quite good.

If the threshold value was set as 20%, the modulation process would be finished in 5 min, but the modulation result could not match the ideal refractive index distribution, and the modulation precision was low. If the threshold value was set as 5% or less, the modulation process would keep on going, which indicated that the LC phase modulator could not achieve this precision. In the experiment, we set the threshold value as 10% when the process time is 10 min. In order to compare the modulation time of the adaptive modulation system with the traditional method, the MAPE value of traditional method was set as 10%. Compared with the traditional modulation method, which at least need several hours, with the adaptive system, the modulation process could be finished in 10 min. The modulation time only needs about 10% of the conventional modulation process time. A graded refractive index (GRIN) lens is widely applied in LC devices because its refractive index distribution can be fitted to the ideal lens[13]. Figure 5(a) shows the simulation result of the transmittance distribution of an ideal GRIN lens. The MAPE of the measured transmittance distribution before modulation was about 20%, as shown in Fig. 5(c). The MAPE of the measured transmittance distribution after modulation was about 10%, as shown in Fig. 5(d). After modulation, the transmittance distribution is much closer to the ideal distribution. Therefore, with the adaptive system, the MAPE of the transmittance distribution of the LC phase modulator can be much improved.

The refractive index distribution of the LC phase modulator can be obtained by using the measured transmittance distribution, as shown in Fig. 6. Compared with the refractive index distribution before modulation, the distribution after modulation is much closer to the ideal distribution. The result demonstrates the effect of the adaptive modulation system.

The error function (EF)[18] was introduced to evaluate the aberration of the ideal refractive index distribution and the measurement refractive index distribution before and after modulation. It can be calculated by
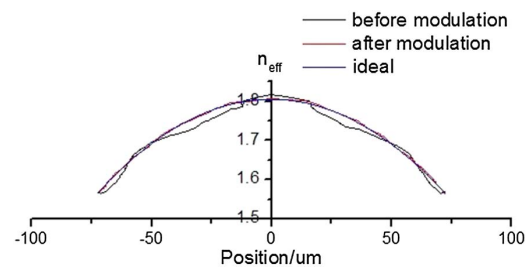

Fig. 6. Ideal refractive index distribution and measurement refractive index distribution before and after modulation.

$$EF = \sqrt{\sum (S_i - P_i)^2 / D} \times 100\%, \qquad (4)$$

where S_i is the measured phase profile of the LC phase modulator, P_i is the ideal phase profile, and D is the aperture size. By our calculation, the EF before and after modulation was 2.71% and 0.25%, respectively. Compared with the refractive index distribution before modulation, the mean square deviation of the refractive index distribution after modulation is significantly decreased by using the adaptive modulation system, which means the refractive index distribution after modulation can match the ideal distribution well.

In this Letter, an adaptive modulation system is demonstrated to automatically modulate the driving voltage of an LC phase modulator. By using the system, the refractive index distribution of the LC phase modulator can be modulated very close to the ideal profile, and a low EF of 0.25% can be achieved in a short modulation time, less than 10% of that by using conventional modulation method. The adaptive modulation system shows potential applications for three-dimensional displays, free-space light modulators, and communication devices.

References

1. J. Zhang, J. S. Nelson, and Z. P. Chen, Opt. Lett. **30**, 147 (2005).
2. J. Leng, X. Sang, and B. Yan, Chin. Opt. Lett. **12**, 040301 (2014).
3. L. Gao, J. J. Zhang, X. F. Chen, and J. P. Yao, IEEET. Microwave Theory. **62**, 380 (2014).
4. F. Gonte, A. Courteville, and R. Dandliker, Opt. Eng. **41**, 1073 (2002).
5. E. Alon, V. Stojanovic, J. M. Kahn, S. Boyd, and M. Horowitz, in *IEEE Global Telecommunications Conference* (2004).
6. C. Liu, D. Wang, L. Yao, L. Li, and Q. Wang, Chin. Opt. Lett. **13**, 082301 (2015).
7. Y. Zhang, F. Z. Zhang, and S. L. Pan, Photon. Res. **2**, 143 (2014).
8. E. R. Dufresne, G. C. Spalding, M. T. Dearing, S. A. Sheets, and D. G. Grier, Rev. Sci. Instrum. **72**, 1810 (2001).
9. J. E. Curtis, B. A. Koss, and D. G. Grier, Opt. Commun. **207**, 169 (2002).
10. Z. Song, Y. Yu, X. Zhang, Z. Wei, and Z. Meng, Chin. Opt. Lett. **12**, 090606 (2014).
11. R. Li, X. Han, X. F. Chen, and J. P. Yao, IEEE. Photon. Tech. Lett. **27**, 1961 (2015).
12. C. W. Chen, Y. C. Huang, and Y. P. Huang, SID Symp. Dig. Tech. Pap. **41**, 428 (2010).
13. J. G. Lu, X. F. Sun, Y. Song, and H. P. D. Shieh, J. Display Technol. **7**, 215 (2011).
14. Y. P. Huang, C. W. Chen, and T. C. Shen, SID Symp. Dig. Tech. Pap. **40**, 336 (2009).
15. Y. P. Huang, L. Y. Liao, and C. W. Chen, J. Soc. Inf. Disp. **18**, 642 (2010).
16. M. Hain, R. Glöckner, S. Bhattacharya, D. Dias, S. Stankovic, and T. Tschudi, Opt. Commun. **188**, 291 (2001).
17. L. G. Commander, S. E. Day, and D. R. Selviah, Opt. Commun. **177**, 157 (2000).
18. R. Zhu, S. Xu, Q. Hong, S. T. Wu, C. Lee, C. M. Yang, C. C. Lo, and A. Lien, Appl. Opt. **53**, 1388 (2014).